JOURNAL OF APPLIED ELECTROCHEMISTRY 24 (1994) 1037–1043

A composite electrode for studying powdered electroactive materials: preparation and performance

M. KEDDAM, S. SENYARICH, H. TAKENOUTI

UPR 15 du CNRS "Physique des Liquides et Electrochimie", Tour 22, 4 Place Jussieu, 75252 Paris Cedex 05, France

P. BERNARD

SAFT, AAR, Route de Nozay, 91460 Marcoussis, France

Received 12 November 1993; revised 3 March 1994

An advance in Ni–Cd rechargeable battery technology is being achieved by introducing positive active material made of pasted nickel hydroxide spherical particles (SP) into a nickel foam. The performance of this kind of electrode, and particularly its improved volumic capacity, are determined by several technological factors, the contributions of which are difficult to dissociate. A composite electrode was prepared by electrodeposition of nickel from a $Ni(OH)_2$ particle suspension in a Watts' bath. A single layer of particles was partly embedded in the nickel coating grown on a nickel support. It is shown that the contribution of the metallic nickel matrix is negligibly small in both kinetic and spectroscopic responses of the electrode, hence allowing the behaviour of the nickel hydroxide particles to be investigated.

1. Introduction

The nickel hydroxide/nickel oxyhydroxide couple is the main redox system used in the positive electrode of alkaline batteries. The reversibility and cyclic behaviour of this electrode is good. To increase the volumic efficiency of the active material, a new technology based on a 'foam' electrode was recently introduced [1–4]. The active material, nickel hydroxide spherical particles (SP) in a pasted form, is packed into highly porous metallic nickel matrix. The latter works as an electrical collector (connection between the SP and the external circuit). The whole system offers greater volumic capacity than sintered technology because the quantity of metallic nickel is reduced.

The behaviour of the SP industrial electrodes may involve different interactions such as SP–SP contacts, SP–nickel foam contacts and transport limitations inside the bulk electrode. Consequently, it is difficult to determine the intrinsic kinetic and electrochemical behaviour of the nickel hydroxide SP. To avoid these complications, a composite electrode was made by embedding the SP into an electrodeposited coating of metallic nickel. After establishing the electrochemical contribution of metallic nickel, it was possible to investigate the electrochemical behaviour of the SP at the granular scale by cyclic voltammetry, impedance measurements, Raman spectroscopy and X-ray diffraction.

2. Preparation of the composite electrode

SP of nickel hydroxide supplied by Tanaka Inc. (diameter 20 μm) were maintained in suspension in a Watts' bath by a magnetic stirrer. The bath composition [5] is given in Table 1.

The bath temperature was controlled near 50 °C and about five volume percent of SP was added. The SP were first maintained in suspension for a few seconds by a magnetic stirrer. A nickel disc electrode (Johnson Matthey) facing upward was then introduced into the bath after stopping the magnetic stirrer. The SP were then allowed to deposit on the electrode surface by sedimentation from the stagnant electrolyte.

Simultaneously a cathodic current of 3 A dm^{-2} was applied and metallic nickel was deposited on the patches of the surface not in contact with the SP. Consequently, a composite layer was grown in which the nickel hydroxide particles were embedded as sketched in Fig. 1.

The thickness of the nickel layer was monitored to incorporate only a single or several SP layers using Faraday's law. The faradaic efficiency of electrodeposition was close to unity without SP, as determined by weighing a nickel deposit on a 25 μm nickel sheet. In contrast, the current efficiency fell to 2/3 when the SP were present on the electrode surface (calculated from the thickness of deposit nickel layer estimated on SEM pictures). A similar current efficiency (2/3) was obtained with glass or SiC particles i.e. one third of the current was not used for cathodic reduction of the Ni^{2+} but most likely for hydrogen evolution. This process might take place preferentially at the SP/nickel interface where hydrogen overvoltage is expected to be lower than on bulk nickel [6]. The composite electrode thus obtained is illustrated in Fig. 2.

0021-891X

Table 1. Watts' bath composition

$Ni_2SO_4.7H_2O$	300 g dm^{-3}
$NiCl_2.6H_2O$	35 g dm^{-3}
H_3BO_3	40 g dm^{-3}
pH	4.5

3. Characterization of the composite electrode

The first stage of the investigation was to assess whether the chemical (Watts' bath) or electrochemical (cathodic current) conditions prevailing during the electrode preparation had modified the active material (SP). Using microRaman spectroscopy and X-ray diffraction, SP were characterised as delivered and after embedding.

X-ray diffraction spectra were obtained with MoK_α radiation and are shown in Fig. 3(a) (free SP) and 3(b) (embedded SP). If the peaks due to the metallic nickel were subtracted, there would be no change in the X-ray diffractogram which is characteristic of the β-Ni(OH)$_2$ phase. Thus no crystallographic structure change has occurred during the preparation of the composite electrode.

MicroRaman diffusion spectra were obtained using a Dilor multichannel Raman spectrometer, with a 514.5 nm argon laser line, a 50 mW power at LASER output (the power was about a tenth of this value on the sample surface, after crossing over the Raman microscope) and an integration time of 2 s. The spectra are displayed in Fig. 4(a) (free SP) and 4(b) (embedded SP). Those spectra show no frequency shift in the Raman spectra, indicating no chemical change, and are characteristic of the β-Ni(OH)$_2$ phase as identified by X-ray diffraction.

On the basis of both techniques it is concluded that the SP have undergone neither chemical nor structural changes. Moreover, SEM observations showed that the size and the shape of the surface of the SP were not modified during the preparation of the composite electrode.

4. Effect of metallic nickel

Before the application of various techniques for characterising the nickel hydroxide particle behaviour, the response of the electrodeposited nickel alone was investigated in order to determine

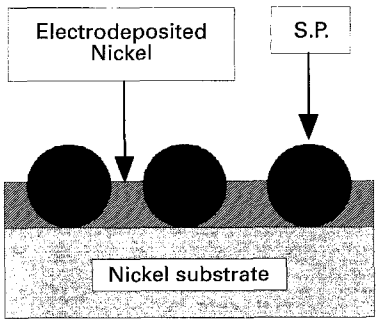

Fig. 1. Nickel hydroxide spherical particles (SP) partly embedded in an electrodeposited nickel coating.

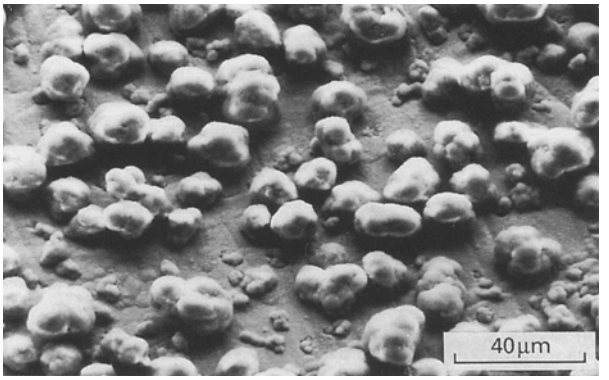

Fig. 2. SEM micrograph of the composite electrode.

to what extent this layer interferes in the characterization of the nickel hydroxide particles.

4.1. *Cyclic voltammetry*

Figure 5 shows voltammograms obtained in 5 M KOH with an electrodeposited nickel electrode alone (curve (a)) and that with the composite electrode (curve (b)) at a sweep rate of 10 mV s^{-1}. The current peak observed on the nickel electrode, 60 μA, is less than one hundredth of that of the composite electrode, 20 mA. Both electrodes were polarised between 0.1 and 0.7 V vs Hg/HgO/5 M KOH reference electrode. The voltammograms shown here were obtained on the 20th cycle.

4.2. *Impedance measurements*

All the impedance measurements presented in this paper were obtained with Schlumberger Solartron equipment (1286) electrochemical interface and 1254

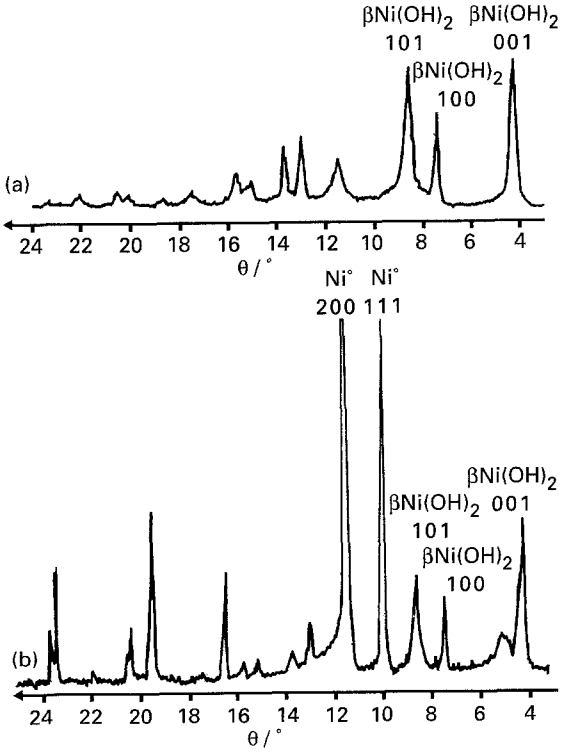

Fig. 3. X-ray diffraction spectra. (a) Free SP, (b) embedded SP.

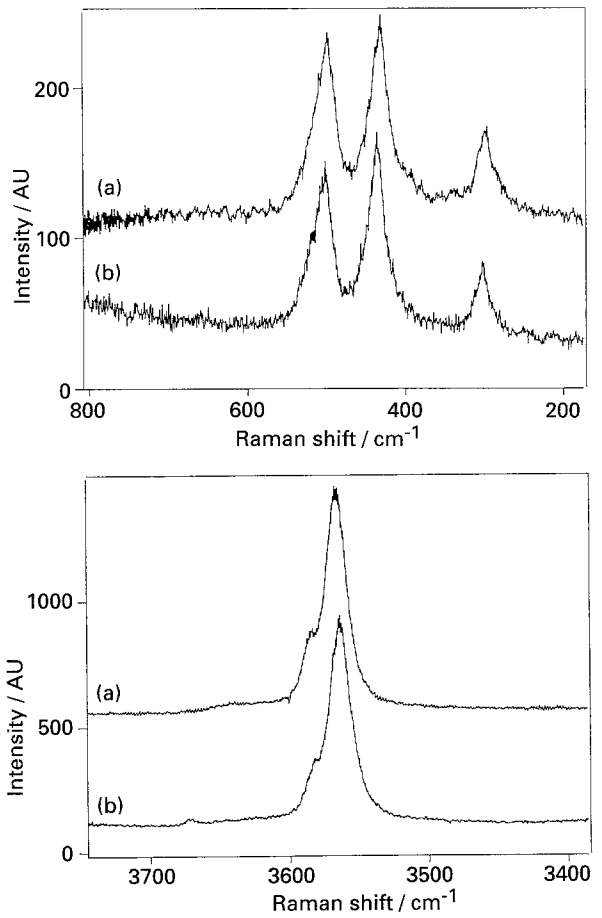

Fig. 4. MicroRaman spectra. (a) Free SP, (b) embedded SP.

frequency response analyser) coupled with an analog filter (Kemo VBF8). The experiments were monitored by Fracom 2.1 software developed in this laboratory. Two 0.2 cm^2 surface electrodes, a nickel electrode and a composite electrode were prepared. Both were cycled ten times in 5 M KOH between 0.1 and 0.6 V at a sweep rate of 1 mV s^{-1}.

This preliminary cycling is necessary to activate the whole of each SP. Both electrodes were set at 0.25 V (reduced state) for 15 min to obtain a steady-state current, then the impedance measurements were carried out from 63.5 kHz to 0.1 mHz.

Comparison of the diagrams, Fig. 6(a) and (b), shows that the impedance of the electrodeposited nickel electrode is about 50 times greater than that of the composite electrode.

Both contributions from electrodeposited nickel and SP being considered to take place in parallel (50/50 surface coverages), the SP impedance is equal to the composite electrode impedance with an approximation of about 1%.

4.3. *Micro-Raman spectroscopy*

Though the area analysed by this technique (1 μm^2) is sufficiently small to focus at the centre of a SP (diameter 20 μm), it was important to confirm that the Raman response of the electrodeposited nickel (reduced or oxidized state) was negligible, as shown in Fig. 7.

4.4. *X-ray diffraction*

With the purpose of studying the nature of the oxidation products of the SP, it was important to verify that the metallic nickel peaks were sufficiently well separated from those of the nickel hydroxide and the nickel oxyhydroxide. As expected from the data found in ASTM tables, nickel does not interfere in the relevant zone, where θ (with MoK_α radiation) is smaller than 10° (Fig. 3).

5. Electrochemical behaviour

After having established that the nickel contribution was negligible it was possible to study the electrochemical behaviour of the SP themselves.

5.1. *Cyclic voltammetry*

The composite electrode was cycled between 0.1 and 0.7 V vs Hg/HgO/5 M KOH reference electrode with a sweep rate of 10 mV s^{-1}. The electrolyte was 5 M KOH.

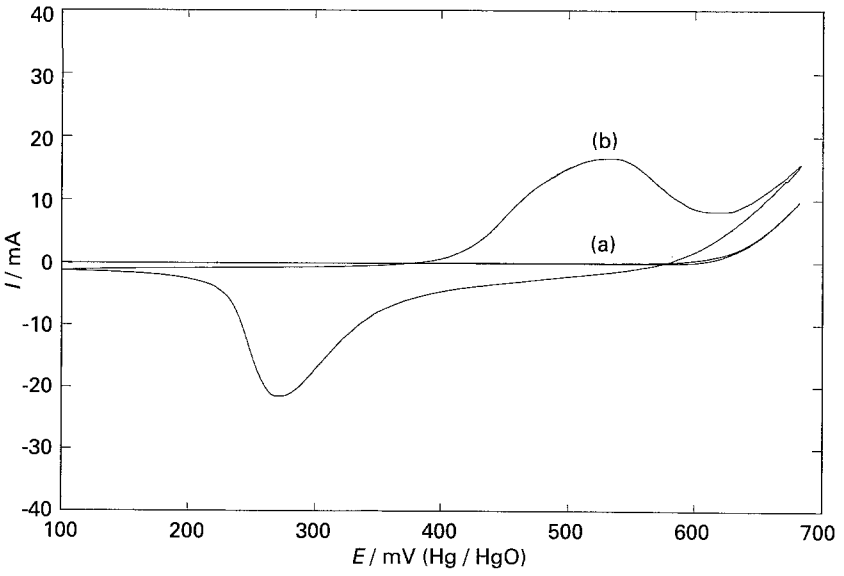

Fig. 5. Cyclic voltammograms (cycle 20). (a) Electrodeposited nickel, (b) composite electrode. Scan rate: 10 mV s^{-1}.

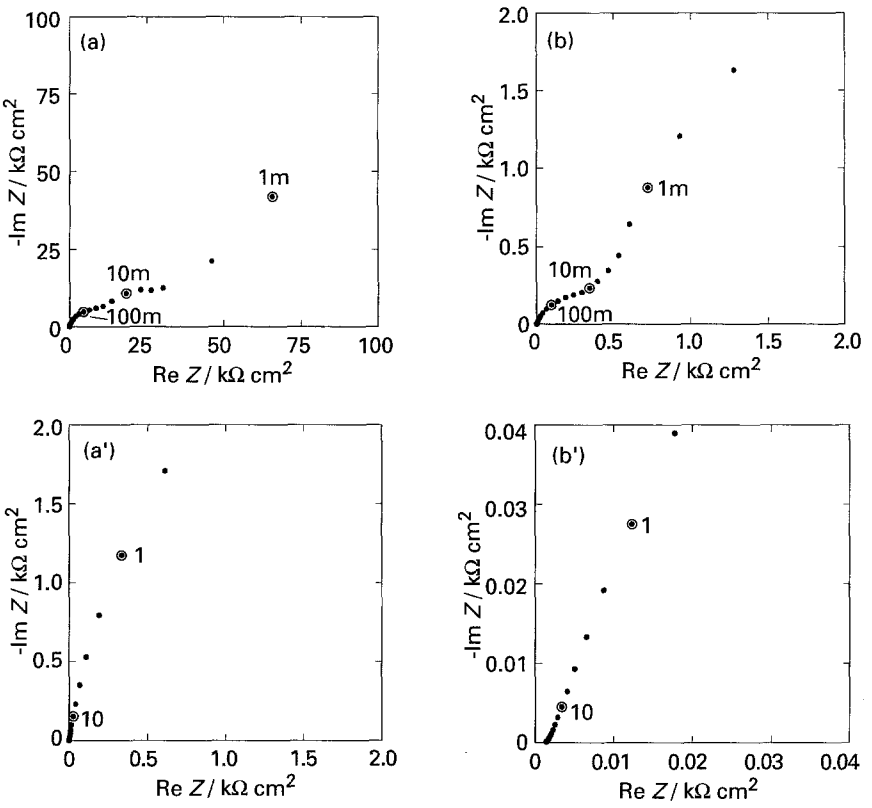

Fig. 6. Impedance measurements. (a) Electrodeposited nickel, (b) composite electrode. (a′) and (b′) diagrams are close-up view of the high frequency range.

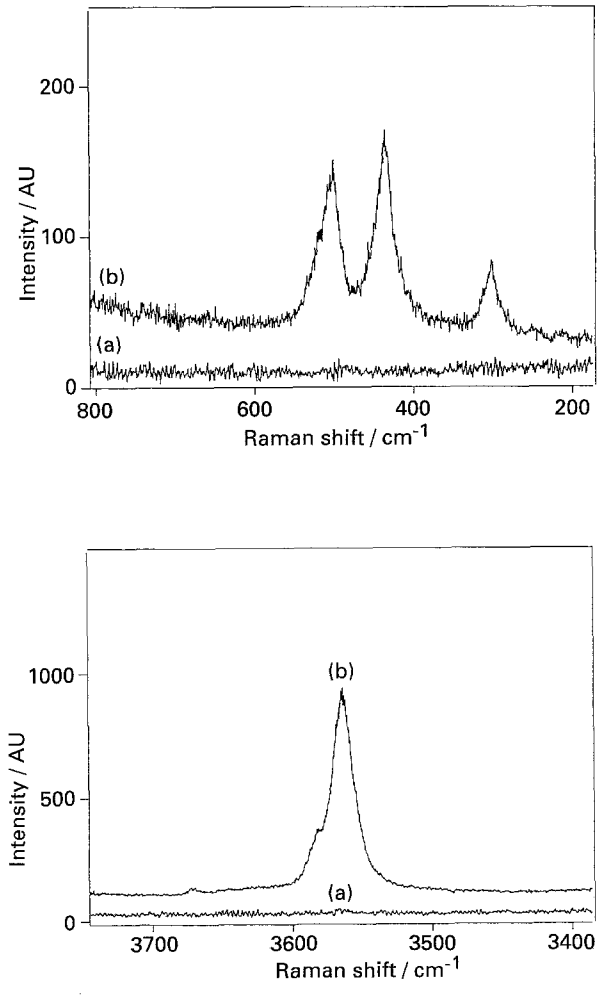

Fig. 7. MicroRaman spectra. (a) Electrodeposited nickel (reduced or oxidized); (b) uncycled composite electrode.

The oxidation peak is broad and located at about 0.5 V. At potentials more anodic than 0.6 V, a current increase due to oxygen evolution is observed. However, the current peak relative to the oxidation of nickel hydroxide and I/E characteristics for oxygen evolution are hardly separated. This overlapping of the two characteristics is very marked during the first potential sweep, and no marked peak due to the oxidation of nickel hydroxide is seen.

However, the oxidation reaction took place as indicated by the first reverse cycle with a reduction peak at about 0.3 V. For the subsequent cycles, the SP oxidation peak potential is lower and can be partly observed. The reduction peak is also broad and is located at about 0.25 V.

The important feature on the voltammograms of Fig. 8 is the gradual increase in the exchanged charge with the number of cycles. The charge reaches its maximum value at about the 20th cycle. Figure 9(a) illustrates this evolution of the exchanged charge with respect to the cycle number. In these experiments, the metallic nickel thickness was chosen to embed the SP up to their half-height (10 μm).

These results are in agreement with a model shown in Fig. 9(b) assuming that at any cycle, a constant thickness of the SP is freshly transformed. During the first cycle, the reaction propagates from the $Ni/Ni(OH)_2/KOH$ interface (where both electronic and ionic phases are in contact) towards the $Ni(OH)_2/KOH$ interface (because the SP contain no electrolyte). The skin of the SP having been cycled (it is now conductor and impregnated with electrolyte), the second cycle, also taking place at

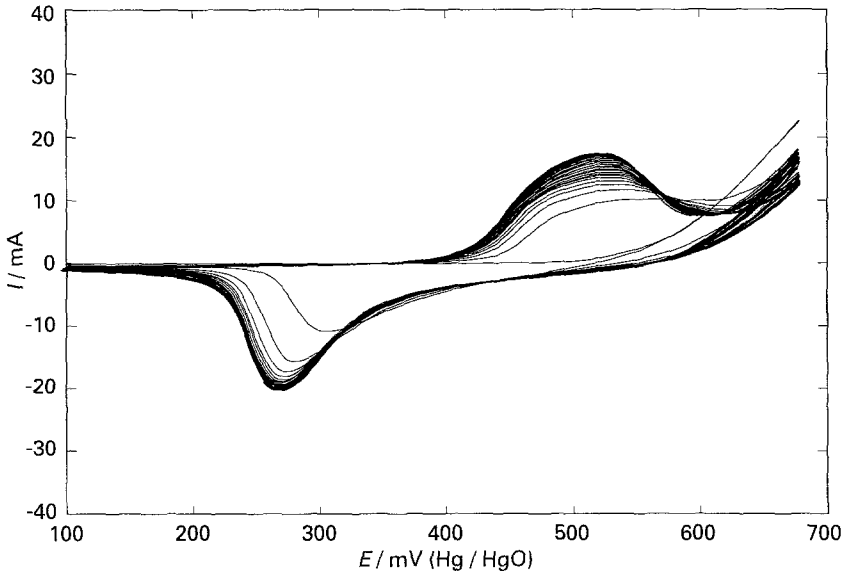

Fig. 8. Cyclic voltammograms of a composite electrode (first 30 cycles).

the $Ni/Ni(OH)_2/KOH$ interface, will involve a deeper thickness of the SP. This cycle is repeated each cycle causing the first transformation of a new thickness, up to the centre of the SP.

Figure 10 shows the SEM micrograph of the cross section of a composite electrode with two layers of SP. On the one hand, the outer layer (right side) in contact with KOH has been transformed during the cycling. On the other hand, the inner layer (left side) completely embedded in nickel was not activated. This picture does not show a state of partially charged electrode but a fully charged electrode at a given stage (30 cycles) of its progressive cycle-by-cycle activation. In that sense it cannot be compared to the propagation of the reacting front from the nickel substrate towards the KOH solution [7].

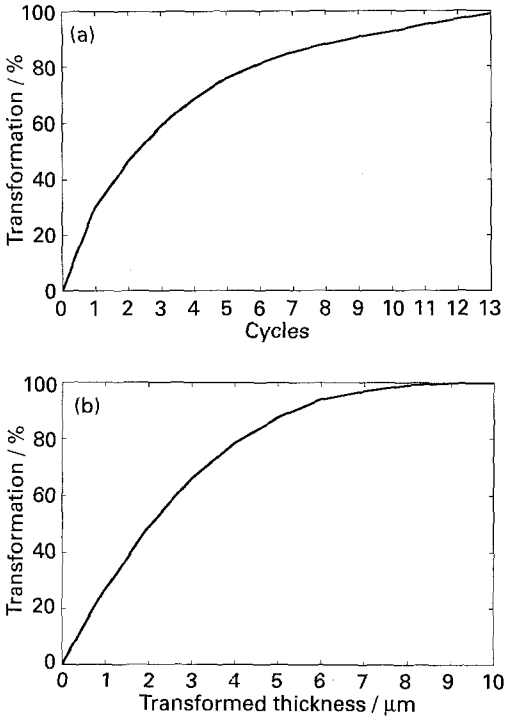

Fig. 9. (a) Evolution of the exchanged charge with the number of cycles (sweep rate $10\,mV\,s^{-1}$). (b) Calculated results for a model of a radial inwards propagation of the reaction.

5.2. *Impedance measurements*

Impedance measurements were performed with the same material, in the same frequency range, and after the same SP preactivation procedure, as mentioned previously. The measurements were performed from 0.1 to 0.7 V at a series of potential values separated by a 50 mV step and then back from 0.7 to 0.1 V with the same voltage stepping. After each potential increment, the electrode was set at this potential for 15 minutes to obtain a steady-state current. The software controlled these entire sequences automatically. The Nyquist diagrams were obtained for a $0.2\,cm^2$ geometrical area but the extended surface area of the SP measured with the BET method was about a hundred times as large.

5.2.1. Reduced state. The Nyquist diagrams shown in Fig. 11(a) depict two RC loops. The electrical parameters were fitted with a program using the simplex method. The capacitance associated with the HF loop ($f > 0.01$ Hz) can be attributed to the double layer since the parallel capacitance of this loop is evaluated to be 20 to $30\,\mu F\,cm^{-2}$ when referred to the extended surface. The HF resistance may be associated to the ohmic resistivity of the electrode material (SP) as proposed by Bernard [8]. This resistance decreases sharply when the potential goes through the oxidation peak of the SP. It is known that nickel oxyhydroxide is a much better electrical conductor than nickel hydroxide.

5.2.2. Oxidized state. The very small value of the ohmic resistance of the SP does not allow observation of the HF loop. The impedance displays a blocking electrode behaviour as shown in Fig. 11(b).

6. Conclusion

A new technique has been devised for preparing a composite electrode material by codeposition on a metallic nickel support of nickel hydroxide particles

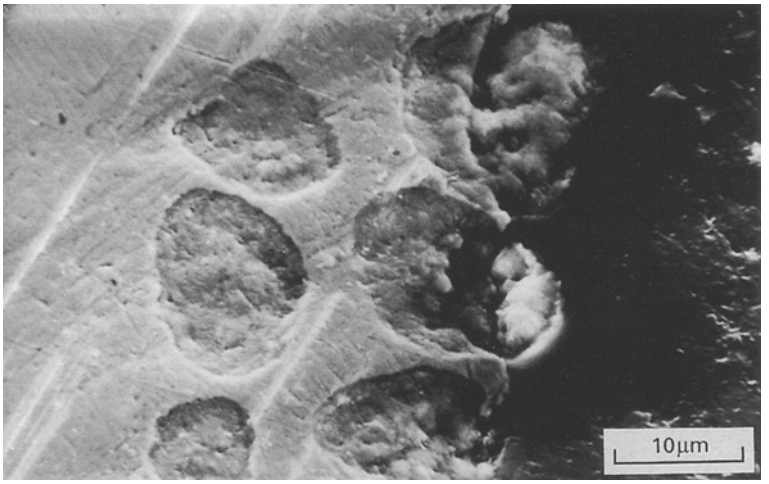

Fig. 10. SEM micrograph of a cross-section of SP after 30 cycles. Right side: electrolyte; left side: nickel coating.

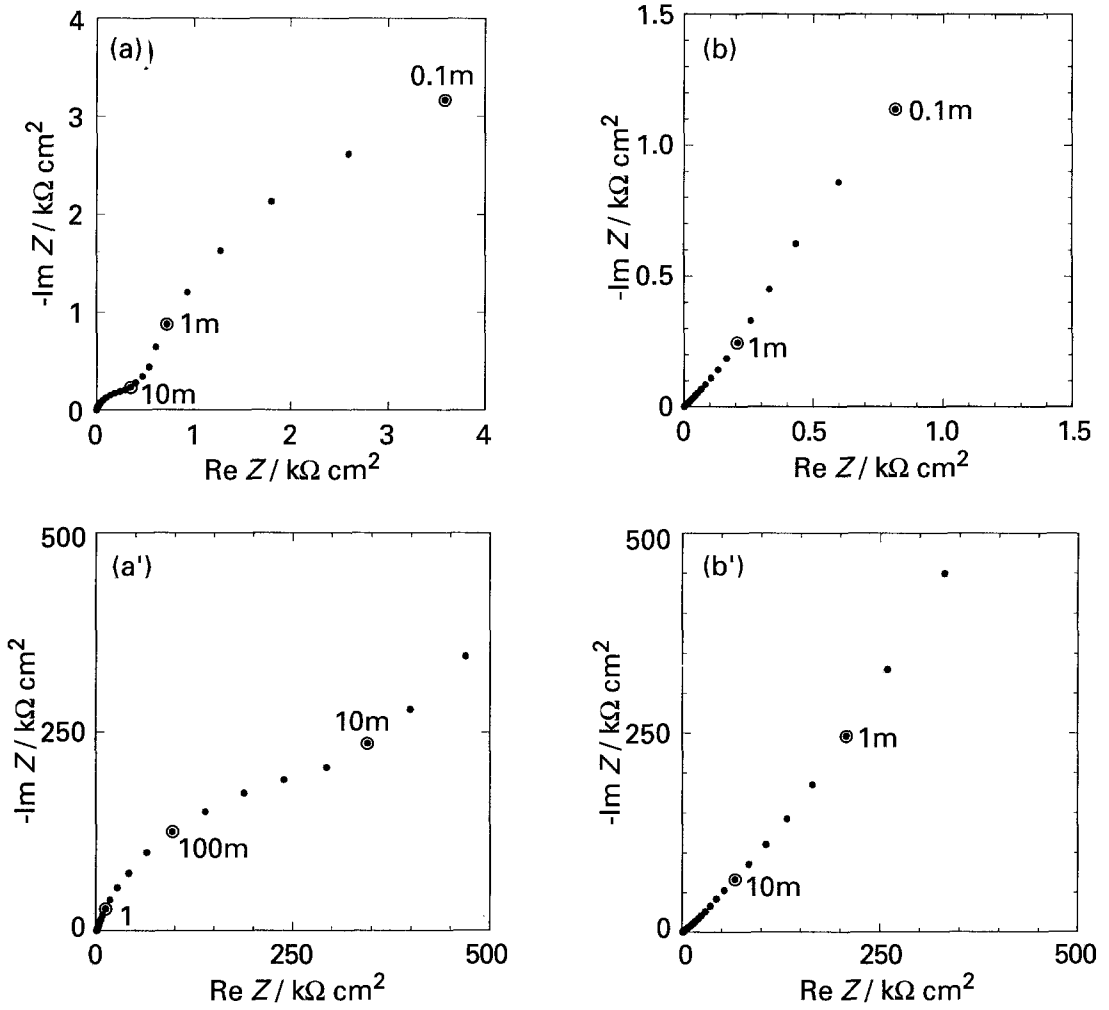

Fig. 11. Impedance measurements. (a) Reduced state (250 mV), (b) oxidized state (450 mV). (a′) and (b′) diagrams are close-up view of the high frequency range.

partly embedded in an electrodeposited nickel coating. It is verified, on the basis of preliminary results, that the electrochemical behaviour of this electrode is completely determined by the nickel hydroxide reactivity itself because the contribution of electrodeposited nickel is negligibly small. This kind of electrode shows promise for a wide range of kinetic and spectroscopic investigations of the electrochemistry of any powdered material, since the electrode thus prepared avoids interference of grain to grain contact resistance, and also significantly decreases the influence of transport phenomena on the bulk electrode kinetics.

Acknowledgement

The authors wish to thank the ANRT for partial financial support of this work.

References

[1] M. Oshitani, H. Yufu, K. Takashima, S. Tsuji and Y. Matsumaru, *J. Electrochem. Soc.* **136** (1989) 1590.
[2] M. Watada, M. Ohnichi, Y. Harada and M. Oshitani, *Yuasa-Jiho* **70** (1990) 4.
[3] Matsushita, *Patent JP 7793* (19.01.83).
[4] J. Babjak, V. A. Ettel, M. A. Mosoiu and P. Kalal, Extended Abstracts of the Electrochemical Society, Fall Meeting, New Orleans, Louisiana, **2** (1993) 100.
[5] Watts, *O.P. Trans. Electrochem. Soc.* **29** (1916) 395.
[6] S. W. Watson, *J. Electrochem. Soc.* **140** (1993) 2235.
[7] G. W. D. Briggs and M. Fleischmann, *Trans. Faraday Soc.* **67** (1971) 2397.
[8] P. Bernard, Thesis, Université Paris 6 (1992).